Elemental analysis by NMR.

AUTHOR(S):

Takeda, Kazuyuki; Ichijo, Naoki; Noda, Yasuto; Takegoshi, K

CITATION:

Takeda, Kazuyuki ...[et al]. Elemental analysis by NMR.. Journal of magnetic resonance 2012, 224: 48-52

ISSUE DATE:

2012-11

URL:

http://hdl.handle.net/2433/189440

Elemental Analysis by NMR

Kazuyuki Takeda [a,*], Naoki Ichijo [a], Yasuto Noda [a],

K. Takegoshi [a],

[a] *Division of Chemistry, Graduate School of Science, Kyoto University, 606-8502 Kyoto, Japan*

Abstract

We explore the possibility for elemental analysis by NMR. To keep the efficiency of the signal acquisition common for all spin species, we propose to fix the frequency and vary the magnetic field to cover the isotopes involved in a sample. We introduce constant-frequency receptivity for quantitative elemental analysis in the frequency-fixed NMR experiment. Field-variable NMR experiments are demonstrated using a cryogen-free superconducting magnet. In addition to elemental analysis in liquid solution, solid-state NMR under magic-angle spinning is also described.

Key words: NMR; elemental analysis; receptivity; constant-frequency receptivity (CFR); field-variable superconducting magnet

* corresponding author
Email address: takezo@kuchem.kyoto-u.ac.jp (Kazuyuki Takeda).

1 Introduction

To analyze the composition of atoms in unidentified materials of chemical interest, a number of elemental analysis techniques have been established[1]. They include combustion method, Atomic Absorption Spectrometry (AAS)[2], Electron Probe MicroAnalyser (EPMA)[3], Electron Spectroscopy for Chemical Analysis (ESCA)[4], Inductively Coupled Plasma (ICP), Secondary Ion Mass Spectrometry (SIMS)[5], and so on. In most techniques, the sample is destroyed by the measurement, except for EPMA, which, however, can only analyze the elements on solid surfaces. Currently, there is no convenient way of nondestructive elemental analysis of bulk samples that include living organisms. In this work, we explore the possibility of complementing these existing techniques by NMR spectroscopy.

The NMR elemental analysis that we propose here can be categorized into those observing isotopes. The isotopes can be identified by their mass number. For radioactive isotopes, radiation from the material and its decaying profile tell their existence. NMR enables us to access another important attribute of the isotope: the spin. There are many atomic elements possessing the spin. Each has a specific gyromagnetic ratio γ, giving the magnitude of the nuclear Zeeman interaction according to $\omega_0 = -\gamma B_0$, where B_0 and ω_0 is the magnetic field and the Larmor frequency. Hence, by observing the NMR signal at ω_0, one can tell the existence of an atom with γ.

Here, we aim at verifying the existence of the nuclear spin species in the sample of interest from a set of NMR measurements covering the resonance conditions. In the conventional NMR system using a high-field superconduct-

ing magnet, one encounters practical difficulties toward this goal. That is, in order to realize the resonance conditions of a number of different spin species, it would be necessary to vary the resonance frequency of the NMR probe circuit. However, retuning or replacement of the radiofrequency (rf) circuit would be quite tedious and elaborate. Even though one endures to do it, quantitative comparison of the signal intensities of different spin species becomes difficult. One solution may be to employ a non-resonant transmission line probe that enables broadband excitation and detection[6], in which one still have to calibrate the frequency responses of the other rf circuits, such as filters, mixers, and so on.

In this work, we adopted an unconventional option of fixing the resonance frequency and varying the external magnetic field. As shown below, this allows quantitative NMR measurement of different spin species. For the variable external field, an electromagnet using iron cores may be convenient. However, the maximum attainable field is low. It is difficult to vary the field of the superconducting magnets used in the conventional NMR systems. In this work, we therefore employ a cryogen-free, field-variable superconducting magnet. In the following, we describe the principle of NMR elemental analysis and an experimental setup we have developed. Then, we show demonstrations in liquid solution and solid samples.

2 Principle

Using a probe tuned at a frequency $|\omega_0|$, we are to observe NMR signals from a set of nuclear spin species with gyromagnetic ratios γ_k $(k = 1, 2, 3, ...)$ by varying the external field B_{0k}. The resonance condition for the k-th nuclear

spin species is given by

$$B_{0k} = -\frac{\omega_0}{\gamma_k}. \tag{1}$$

In thermal equilibrium at temperature T, the magnetization M_k of the k-th nuclear spin species is represented by the Curie's law as

$$M_k = \frac{N'_k \gamma_k^2 \hbar^2 I_k (I_k + 1) B_0}{3 k_\mathrm{B} T}. \tag{2}$$

Here, k_B is the Boltzmann's constant, and I_k and N'_k are the spin quantum number and the number of the spins in the sample, respectively. Using the number N_k of the atoms and the natural abundance x_k, N_k may be expressed as

$$N'_k = x_k N_k. \tag{3}$$

At the resonance condition (Eq. (1)), Eq. (2) is rewritten as

$$M_k = \frac{-x_k N_k \gamma_k \hbar^2 I_k (I_k + 1) \omega_0}{3 k_\mathrm{B} T}. \tag{4}$$

The NMR signal induced across the terminals of the coil after pulse excitation is given by the time derivative of the magnetic flux penetrating through the loop of the coil. Thus, the signal intensity is proportional to both the magnetization M_k and the frequency ω_0. In the present work, ω_0 is fixed, so that the efficiency of signal transmission from the probe to the preamplifier of the spectrometer is common for all nuclear spin species. For excitation, since the nutation rate is proportional to the gyromagnetic ratio γ_k, the pulse width τ has to be adjusted to $\tau = \theta/(|\gamma_k| B_1)$ to ensure the common tip angle θ of the pulse with an intensity B_1 for all target spin species. The relative signal intensity S_k can thus be determined solely by the magnetization M_k with the present approach, which depends linearly on the gyromagnetic ratio γ_k and

the number N'_k of the spins:

$$S_k \propto N'_k \gamma_k I_k(I_k+1) = x_k N_k \gamma_k I_k(I_k+1). \tag{5}$$

Since γ_k and I_k are constants, the relative number N_k of the nuclear spins in the sample can be calculated straightforwardly from S_k.

For comparison, let us briefly discuss the case of a constant static field, where the thermal magnetization M_k and the Larmor frequency are proportional to γ_k^2 and γ_k, respectively, resulting in the overall signal intensity given by the cube of the gyromagnetic ratio[7]. For this reason, the receptivity D is conventionally defined as[8]

$$D = x_k |\gamma_k|^3 I_k(I_k+1). \tag{6}$$

However, the γ^3-dependence of the signal intensity has to be modified if we take account of the efficiency of the circuit, which depends on the frequency and thereby the gyromagnetic ratio. In contrast, the proposed experiment at a constant frequency leads to unambiguous measurement of the nuclear magnetization, because of the common circuit efficiency. In order to look at how the signal intensity depends on the nucleus, we define constant-frequency receptivity (CFR) D_{CF}, which, in contrast to the conventional receptivity D given in Eq. (6), is represented as

$$D_{\mathrm{CF}} = x_k |\gamma_k| I_k(I_k+1). \tag{7}$$

To compare the frequency-variable and the field-variable experiments, D and D_{CF} are plotted in Fig. 1(a)(b) for several nuclear spin species. In both cases, the vertical scales are normalized to the value for the ^{1}H spins. As well known, the conventional receptivity is the highest for ^{1}H, due to its natural abundance

close to 100%, the largest gyromagnetic ratio γ among the stable isotopes, and the γ^3-dependence of D. In terms of CFR, however, ^{1}H is no longer the most sensitive spin species. Since D_{CF} increases only linearly with γ, the gain with the higher gyromagnetic ratio is much smaller compared to the case of the conventional receptivity. Hence, in the case of D_{CF}, the effect of the $I^2 = I(I+1)$ term becomes important. Indeed, CFRs for many nuclei are higher than that of ^{1}H. For example, ^{23}Na ($I = 3/2$) has a gyromagnetic ratio of 11.270 MHz/T, which is lower than that of ^{1}H (42.577 MHz/T)[8]. However, with the $I(I+1)$ term of ^{23}Na five times higher than that of ^{1}H, the CFR of ^{23}Na is ca. 1.3 times larger than the CFR of ^{1}H.

3 Experimental

Fig. 2(a) shows a diagram of the experimental setup for NMR elemental analysis. In addition to a home-built NMR spectrometer[9–11], a cryogen-free, field-variable superconducting magnet (mCFM-7T-50-H3, Cryogenic Ltd) is equipped. This desktop magnet, shown in Fig. 2(b), has an external refrigerator to keep the temperature of the magnet wire below 4 K. The static field can be varied up to 7 T by heating a part of the wire of the magnet, breaking superconductivity, and altering the electric current flowing through it. On switching the heater off, the magnet begins to operate in the persistent-current mode again. The current and heater are controlled by a host computer via a GPIB interface. Full field-sweep from 0 to 7 T takes several minutes. The computer is also used for command/data communication with the NMR spectrometer.

The nominal field homogeneity of this magnet is ca. 0.1% over the volume of 1 cm^3 at its center. The field distribution over the sample volume is rather

large compared to that in the current typical high-resolution NMR systems. Broadening of the resonance line can obscure the diverse nuclear spin interactions which are otherwise measurable, including chemical shifts, J couplings, and so on. Nevertheless, when the atomic composition alone is of interest, this magnet suffices our purpose, as demonstrated below.

The diameter of the magnet bore was 51 mm. We built two probes with an outer diameter of 50 mm (Fig. 2(c)), one of which was for stationary samples while the other was for magic angle spinning (MAS) experiments. For the static-sample probe, we wound a 6-turn solenoid coil with a diameter of 4 mm and length of 6 mm using a coated copper wire, and made a balanced tank circuit resonating at 30.03 MHz. In the MAS probe, we used a 3.2 mm spinning module (Agilent) tuned at either 75.0 MHz or 106.0 MHz.

4 Results and Discussion

First, we performed an NMR elemental analysis experiment in 5.00 M aqueous solution of sodium dihydrogen phosphate (NaH_2PO_4), aiming at detecting the existence of the ^{1}H, ^{31}P, and ^{23}Na spins in the sample. Fig. 3 shows NMR spectra obtained at a fixed frequency of 30.03 MHz. The first NMR signal was found at 0.7054 T (Fig. 3(a)), which corresponds to the resonance condition of the ^{1}H spin. We also found NMR signals in 1.742 T and 2.665 T (Fig. 3(b) and (e)), which were assigned to be ^{31}P and ^{23}Na, respectively. In addition, NMR signals appeared in 2.477 T and 2.653 T (Fig. 3(c) and (d)). These magnetic fields correspond to the resonance conditions of ^{65}Cu and ^{63}Cu. They were due to the copper nuclei inside the wire of the sample coil, as the signals were detected even without the sample and disappeared when we replaced the

copper wire with a silver wire. We found no other signals in the magnetic fields of up to 7 T. We also measured the empty sample tube as well, and found a ^{1}H background signal. Accordingly, we made a correction in the ^{1}H experiment described below, so that the contribution of the probe background signal to the elemental analysis was not counted.

In the present sample (5.00 M NaH_2PO_4 aq), the molar fractions of the ^{1}H, ^{31}P, and ^{23}Na spins are 24.1:1:1. In order to study the quantitative aspect of NMR elemental analysis, we performed measurements at a fixed frequency of 75.0 MHz and compared the signal intensities. Here, it should be noted that prior knowledge of the spin-lattice relaxation time is required, in order to make sure that the spin system is in thermal equilibrium. This may be verified by examining the signal intensities with various recycling delays of signal accumulation. In the present case, the signal was accumulated with recycle delays of 2.5 s, 7.5 s, and 50 ms, for ^{1}H, ^{31}P, and ^{23}Na, respectively.

In addition, the signal decay due to the spin-spin relaxation time during the receiver dead-time should also be taken into account. In a single pulse experiment, the excitation pulse is to be immediately followed by signal acquisition. In general, however, one has to wait for an interval of the order of ten microseconds. In the present case, the receiver dead time was 20 μs. This was due to the trailing edge of the pulse lasting for $\sim 2Q/\omega_0$. Using the Carr-Purcell-Meiboom-Gill (CPMG) method, we measured the spin-spin relaxation times in the present sample of aqueous solution of NaH_2PO_4 to be 29.9 ms, 228 ms, and 8.98 ms for ^{1}H, ^{31}P, and ^{23}Na, respectively. Since they were much longer than 20 μs, the signal decay during the dead time was negligible.

The measured relative peak-area intensities of the ^{1}H, ^{23}Na, and ^{31}P spectra

was 59.4:3.24:1.00. By dividing these values by D_{CF} (Eq. (7)), we determined the relative amount of the H, P, and Na atoms to be 24.1:0.994:1.00. Here, we repeated the identical experimental operations ten times, and took the average value of the results. The error was estimated from the standard deviation to be 4.1%. The result is in agreement with the expected ratio 24.1:1.00:1.00, confirming that the constant-frequency receptivity introduced in this work is a reasonable measure of the sensitivity for the frequency-fixed, field-variable experiments. The error was caused by the noise. By increasing the number of signal averaging, the signal-to-noise ratio and thereby the accuracy of NMR elemental analysis would be improved. The price to pay would be the longer experimental time.

Next, we carried out NMR elemental analysis of a powder sample of tin phosphide (Sn_4P_3) under MAS. Fig. 4 shows MAS spectra of the ^{31}P, ^{119}Sn, and ^{117}Sn nuclei measured at a fixed frequency of 106.0 MHz and magnetic fields of 6.141 T, 6.621 T, and 6.929 T, respectively. From the measured signal intensities, we determined the ratio of the numbers of the nuclei to be 10.1:1.10:1.00 for the ^{31}P, ^{119}Sn, and ^{117}Sn spins. The error was estimated to be 5.3%. This is also consistent with the theoretical value of 9.77:1.12:1.00.

We chose to measure tin phosphide, as it is a candidate for a negative electrode in lithium-ion batteries[12]. It attracts interest, because both P and Sn are electroactive to Li. Thus, stoichiometric studies on the electrochemical reaction of tin phosphide with lithium are of importance. We showed that the present approach of NMR elemental analysis would be suitable for quantifying Li, P, and Sn nuclei in the electrode during the charge/discharge processes.

It is worth mentioning that the gyromagnetic ratio of ^{31}P is positive, whereas

those of ^{119}Sn and ^{117}Sn are negative. Since the configuration of the spectrometer was the same throughout the elemental analysis experiment, the issue on how the sign of gamma and that of the radio-frequency phase affect the relative sign of the spectral intensities of positive and negative γ is delicate and can cause problems. Levitt gave in-depth explanation[13] that the sense of the sign of the rf phase changes with that of the gyromagnetic ratio. In the present case of the simple single-pulse experiment, we found no apparent problem with the phase of the spectra of the positive and negative nuclei, as demonstrated in Fig. 4. However, it is important to keep this point in mind. In general, it is safe to follow the instructions recommended by Levitt and Johannessen[14], in particular when NMR elemental analysis is combined with multiple-pulse experiments.

In principle, extension of NMR elemental analysis to diverse solid samples is straightforward. In practice, however, one should keep the following difficulties and limitations in mind. In solids, the anisotropic interactions can broaden the resonance line considerably, and it would be important to make sure that all spin packets are within the excitation bandwidth of the pulse. One may encounter the case in which the resonance line is too broad to be excitable at a time. For nuclei with large chemical shifts or Knight shifts, such as ^{207}Pb, ^{199}Hg, ^{195}Pt, and so on, even isotropic shift distribution can exceed the width of rf pulse excitation. In such cases, quantitative analysis would become unreliable. One may, nevertheless, be able to tell the existence of the isotope. There is another possible problem associated with the large shifts. For a pair of such spin species that their gyromagnetic ratios are close to each other, their spectral ranges can overlap. For unknown samples, it would be difficult to distinguish which species the resonance peak belongs to.

In ^{1}H-rich organic materials, it is common to apply decoupling rf irradiation to the ^{1}H spins, when one measures the NMR signal of other spin species. However, double resonance experiments are outside the scope of the present work where the magnetic field is varied.

For nuclei with half-integer spins, the pulse width giving the maximum transverse magnetization depends on the magnitude of the interaction[15–17]. Thus, it would be difficult to retain the quantitative feature. Conversely, one may take advantage of the diversity of the spin interactions in solids, in order to filter out the nuclear spins being subjected to specific spin interactions. In solution, the signals due to the satellite transitions can be significantly broadened beyond detection.

5 Summary

In this work, we have shown a new approach to elemental analysis using NMR, which allows one to access information as to the existence of atomic nuclei possessing spin. The condition for detecting the signal of a certain nuclear spin species depends on whether the combination of the carrier frequency and the magnetic field satisfies Eq. (1). Thus, one can distinguish the different spin species by making NMR measurements at a fixed frequency for various magnetic fields. The field switching over a wide range has become feasible using a field variable, cryogen-free superconducting magnet. The advantages of the variable static-field experiments are (i) probe re-tuning is not necessary. (ii) Thereby, the efficiency of signal transmission/detection can be fixed throughout the experiment. (iii) Furthermore, the Zeeman energy separation is the same for all spin species at resonance, giving the common Boltzmann popula-

tion distribution over the Zeeman levels. The relative signal intensities simply depend on the spin quantum number and the amount of the spins involved in the sample.

We introduced constant-frequency receptivity (CFR), which is a convenient measure of the signal intensity per unit number of the spins. In this definition, CFR for ^{1}H can be less than those for nuclei having the larger spin quantum number. This prediction has been confirmed experimentally.

The nondestructive nature of NMR is a unique feature that is not found in other existing elemental analysis methods, and would thus find interest in biology, geology, and material science, where noninvasive or in-situ measurement is essential. Extension of the present work to NMR imaging would also be of wide interest. These works are in progress and will be presented elsewhere.

Acknowledgements

This work was supported by Grant-in-Aid for Challenging Exploratory Research (No. 24655010) of Japan Society for the Promotion of Science (JSPS).

References

[1] Alexis Volborth, *Elemental analysis in geochemistry*, Elsevier (1969).

[2] M. S. Cresser, L. C. Ebdon, C. W. McLeod and J. C. Burridge, J. Anal. At. Spectrom. **1** (1986) 1R-17R.

[3] L. S. Birks, *Electron probe microanalysis*, Interscience Publishers (1963).

[4] D. Briggs and M.P. Seah, *Practical Surface Analysis by Auger and X-ray, Photoelectron Spectroscopy*, Wiley (1983).

[5] K.F.J. Heinrich, D.E. Newbury, proceedings of a Workshop on Secondary Ion Mass Spectrometry and Ion Microprobe Mass Analysis held at the National Bureau of Standards (1974).

[6] E. Scott, J. Stettler and J.A. Reimer, J. Magn. Reson. **221** (2012) 117–119.

[7] A. Abragam, *Principles of Nuclear Magnetism*, Oxford (1961).

[8] R.K. Harris, E.D. Becker, S.C. de Menezes, R. Goodfellow, P. Grangere, Pure and Applied Chemistry, **73** (2001) 1795–1818.

[9] K. Takeda, Rev. Sci. Instrum., **78** (2007) 033103.

[10] K. Takeda, J. Magn. Reson., **192** (2008) 218–229.

[11] K. Takeda, Annual Reports on NMR Spectroscopy **74** (2011) 355–393.

[12] B. León, J.I. Corredor, J.L. Tirado, C. Pérez-Vicente, J. Electrochem. Soc. **153** (2006) A1829–A1834.

[13] M.H. Levitt, J. Magn. Reson. **126** (1997) 164–182.

[14] M.H. Levitt, O.G. Johannessen, J. Magn. Reson. **142** (2000) 190–194.

[15] C.S. Yannoni, R.D. Kendrick, J. Chem. Phys. **74** (1981) 747–749.

[16] A. Samoson, E. Lippmaa, Chem. Phys. Lett. **100** (1983) 205–208.

[17] A.P.M. Kentgens, J.J.M. Lemmens, F.M.M. Geurts, W.S. Veeman, J. Magn. Reson. **71** (1987) 62–74.

Figure Captions

Figure 1

(a) The receptivity versus the resonance frequency in a magnetic field of 7 T for several nuclear spin species. The receptivity was calculated according to $x_k|\gamma_k|^3 I_k(I_k+1)$ and normalized by the proton receptivity. (b) The Constant-Frequency Receptivity (CFR) plotted as a function of the resonance field at a constant frequency of 30 MHz.

Figure 2

(a) A schematic diagram of the experimental setup for NMR elemental analysis. It consists of an NMR system and a field-variable, cryogen-free superconducting magnet. The magnetic field is remotely controlled by the computer via a GPIB interface. (b) A snapshot of the system. An OPENCORE NMR spectrometer is used[9–11]. The desktop magnet has a bore with a diameter of 51 mm, and is capable of producing static fields of up to 7 T. (c) A home-built probe. The diameter of the aluminum shield is 50 mm.

Figure 3

NMR spectra obtained in 5.00 M aqueous solution of NaH_2PO_4 at a carrier frequency of 30.03 MHz. The magnetic field was (a) 0.7054 T, (b) 1.742 T, (c) 2.477 T, (d) 2.653 T, and (e) 2.665 T. The peaks were assigned to be ^{1}H, ^{31}P, ^{65}Cu, ^{63}Cu, and ^{23}Na, respectively. The ^{65}Cu and ^{63}Cu signals came from the copper nuclei in the wire of the sample coil. A common receiver gain was used except for the case of ^{1}H, in which the signal was attenuated by 11.0 dB. The signals were accumulated over 3600 times. The pulse delays were 5 s and 10 s for ^{1}H and ^{31}P, and 0.1 s for ^{65}Cu, ^{63}Cu, and ^{23}Na.

Figure 4

MAS spectra obtained in a powder sample of tin phosphide at 106.0 MHz. The spinning frequency was 10 kHz. The signals were accumulated over 200000 times with a recycle delay of 20 ms, 80 ms, and 10 ms for ^{31}P, ^{119}Sn, and ^{117}Sn, respectively.

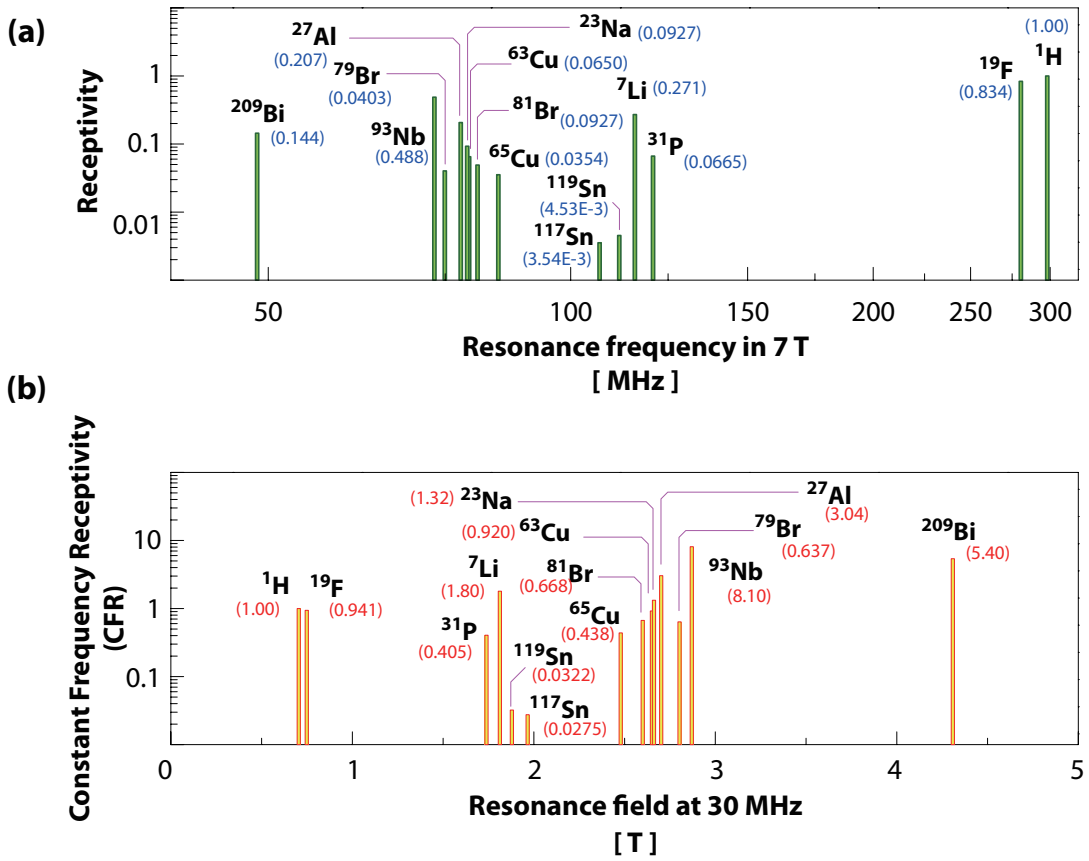

Fig. 1

Elemental analysis...

Takeda et al.

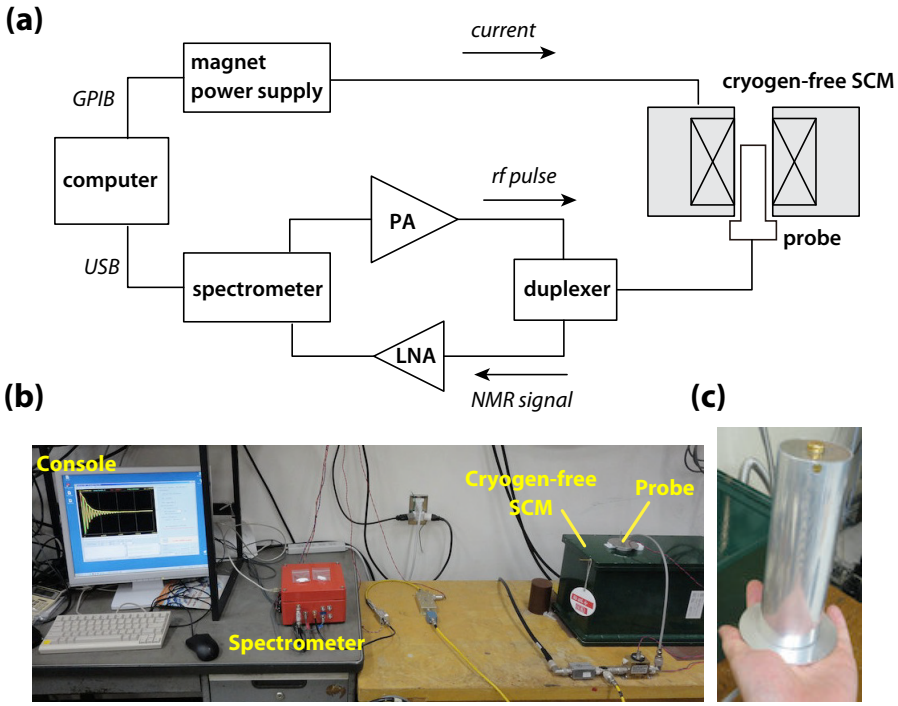

Fig. 2

Elemental analysis...

Takeda et al.

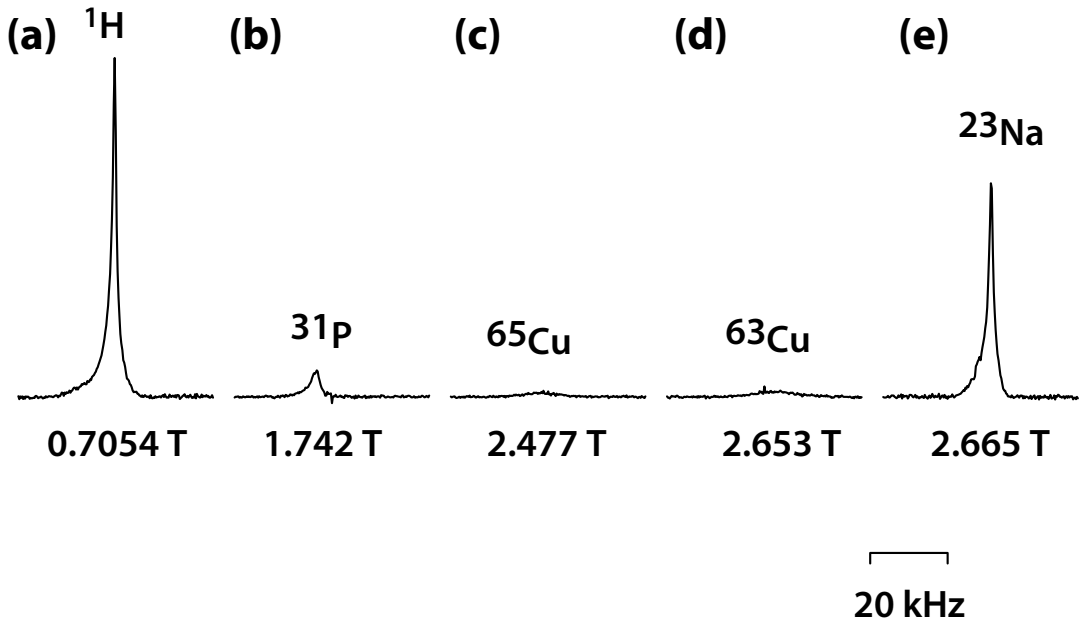

Fig. 3

Elemental analysis...

Takeda et al.

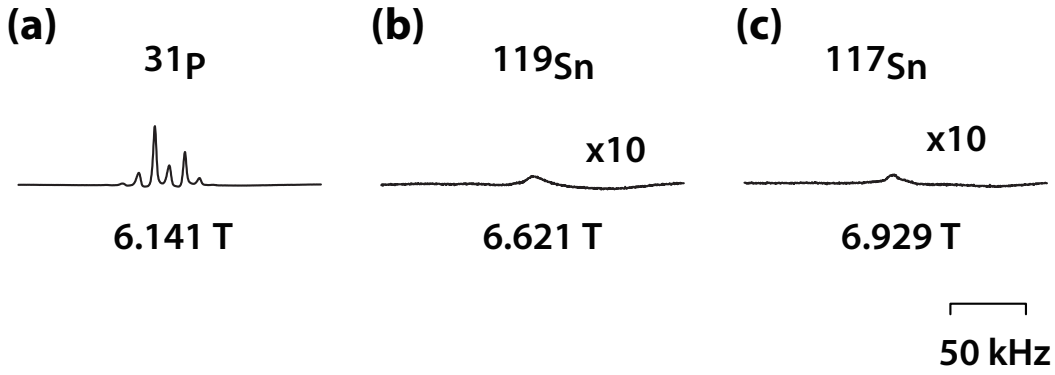

Fig. 4

Elemental analysis...

Takeda et al.